Available online at www.sciencedirect.com
SCIENCE DIRECT®

Journal of Catalysis 238 (2006) 186–195

JOURNAL OF CATALYSIS

www.elsevier.com/locate/jcat

Chemistry of N_2O decomposition on active sites with different nature: Effect of high-temperature treatment of Fe/ZSM-5

Keqiang Sun [a], Haian Xia [a], Emiel Hensen [b], Rutger van Santen [b], Can Li [a,*]

[a] *State Key Laboratory of Catalysis, Dalian Institute of Chemical Physics, Chinese Academy of Sciences, Dalian, 116023, China*
[b] *Schuit Institute of Catalysis, Eindhoven University of Technology, P.O. Box 513, 5600 MB Eindhoven, The Netherlands*

Received 3 August 2005; revised 5 December 2005; accepted 9 December 2005

Abstract

Nitrous oxide decomposition on Fe/ZSM-5 catalysts, prepared by solid-state ion exchange followed by calcination in O_2 at 823 K or high-temperature treatment in He at 1173 K, was studied by steady-state reaction and transient-response techniques. High-temperature treatment induces profound changes in the distribution of iron species, most notably a substantial fraction of oligonuclear and cationic Fe species are converted to Fe species stabilized by extra-framework Al (Fe–O–Al species) in zeolite micropores. Nitrous oxide decomposition is much slower over calcined Fe/ZSM-5 than over its high-temperature-treated counterpart. Only over the latter catalysts is inhibition of N_2O conversion by molecular oxygen observed. Transient response experiments show that molecular oxygen and nitrogen evolve simultaneously for calcined Fe/ZSM-5. It is proposed that the reaction proceeds over isolated Fe^{3+} sites in cationic species or oligonuclear Fe oxide species via a scavenging mechanism in which adsorbed oxygen species react with gaseous nitrous oxide to give molecular nitrogen and oxygen. In contrast, transient-response experiments for the high-temperature-treated catalyst show slow oxygen desorption compared with nitrogen formation, pointing to recombinative oxygen desorption being rate-limiting. This agrees with the finding that the rate is inhibited by molecular oxygen. It is proposed that ferrous ions in the high-temperature-treated catalyst show a much higher reactivity in nitrous oxide decomposition than Fe^{3+} sites. The Fe^{2+} species are most likely associated with the mixed iron and aluminium species formed upon high-temperature treatment.

Keywords: N_2O decomposition; Mechanism; Fe/ZSM-5; Transient-response; Iron species; Active site; Fe–O–Al species

1. Introduction

Nitrous oxide is not only a large source of nitrogen oxides (NO_x) in the stratosphere depleting the ozone layer, but also a strong greenhouse gas with a global warming potential approximately 300 times higher than that of CO_2 [1–3]. Catalytic N_2O decomposition to N_2 and O_2 on Fe/ZSM-5 has received increasing attention recently. Centi et al. [3] and Pérez-Ramírez et al. [4,5] have reported that such catalysts show remarkable activity and stability for nitrous oxide decomposition in the presence of relatively large amount of O_2, H_2O, NO, and SO_2, which are typically poisons for other catalysts used for nitrous oxide abatement. The pioneering works of Panov revealed that nitrous oxide decomposition over iron-containing ZSM-5 zeolite can be used to generate a very efficient oxidant. Nitrous oxide decomposition leaves a reactive α-oxygen species that can oxidize methane and benzene to form methanol and phenol, respectively, even at temperatures as low as 243 K [6]. The oxidation of benzene to phenol with nitrous oxide has received considerable attention because of its potential to replace the current environmentally stressful process for producing adipic acid [7].

Despite the numerous studies relating the structure of these materials to the activity in nitrous oxide decomposition, the exact reaction mechanism is not fully understood. Two mechanisms widely mentioned in the literature share the initial deposition of an oxygen atom from decomposition of nitrous oxide on a vacant iron site [8–13]. In one of these mechanisms, the deposited oxygen atoms react irreversibly with nitrous oxide to form molecular nitrogen and oxygen. In the other mechanism, another nitrous oxide molecule is decomposed over a nearby iron site, and the oxygen atoms recombine to give molecular

---

[*] Corresponding author. Fax: +86 411 84694447.
E-mail address: canli@dicp.ac.cn (C. Li).

0021-9517/$ – see front matter © 2005 Elsevier Inc. All rights reserved.
doi:10.1016/j.jcat.2005.12.013

oxygen. Kapteijn et al. [8] noted that the rate of nitrous oxide decomposition is not inhibited by molecular oxygen and that micromodeling according the first mechanism quantitatively predicts nitrous oxide decomposition. These observations are in favor of the first mechanism. However, a TAP study by the same group [12], as well as the transient-response studies by Pirngruber [9], revealed that the formation of molecular oxygen is always delayed compared with that of molecular nitrogen and that the evolution of oxygen is more diffuse than that of nitrogen. These observations indicate that deposited oxygen atoms are removed by recombination. Both mechanisms have been widely adopted to explain the respective results reported in the literature [10–13].

Iron speciation strongly depends on the method of iron introduction and the subsequent treatments [11,13–21]. The extent of iron clustering greatly affects the activity of iron-containing ZSM-5. In general, high-temperature treatment increases the performance in nitrous oxide decomposition [11,17,18,22–25]. Changes in the kinetic parameters with such treatment have been reported [11]. Moreover, steaming at elevated temperatures also improves the activity and selectivity in benzene oxidation with nitrous oxide. Recently, some of us have suggested that selective phenol formation is catalyzed by a very small number of isolated Fe sites, whereas nitrous oxide decomposition is catalyzed by more clustered iron oxide species [26].

The present work was undertaken to investigate the effect of high-temperature (1173 K) treatment of Fe/ZSM-5 prepared by solid-state ion exchange on the mechanism of nitrous oxide decomposition. Toward this end, the nature of iron sites on Fe/ZSM-5 calcined in O_2 at 823 K and on Fe/ZSM-5 pretreated in He at 1173 K was characterized by UV–vis and infrared spectroscopy. The mechanism and kinetics of N_2O decomposition were studied by steady-state activity measurements and transient-response techniques following the procedures developed by Pirngruber et al. [9,25]

2. Experimental

2.1. Solid exchange of $FeCl_3$ with H-ZSM-5

The sample Fe/ZSM-5 was prepared by a solid-state ion exchange method following the procedure of Karge et al. [27]. Typically, 2 g of NH_4-ZSM-5 (Si/Al = 25, Nankai University) was calcined in pure O_2 flow at 823 K and ground with an appropriate amount of anhydrous $FeCl_3$ in an Ar-flushed glovebox. Then the mixture was heated from room temperature (RT) to 598 K at a ramp rate of 8 K/min in He flow and maintained at this temperature for 2 h. The solid was further treated in a flow of 0.5% H_2O in Ar from RT to 473 K to hydrolysis Fe–Cl bonds. The obtained material was calcined in pure oxygen by heating from RT to 823 K at a ramp rate of 8 K/min, followed by an isothermal period of 2 h to obtain Fe/ZSM-5(C). A portion of calcined Fe/ZSM-5(C) was further treated in He flow at 1173 K for 2 h to obtain Fe/ZSM-5(HT). XRD measurements of Fe/ZSM-5(C) and Fe/ZSM-5 (HT) showed that the MFI structure of the zeolite was not destroyed after high-temperature treatment. The resulting catalysts contain 2.4 wt% iron, corresponding to an atomic $Fe/Al_{framework}$ ratio of 0.66.

2.2. Characterization

Infrared spectra were collected on a Nicolet Impact 410 FTIR spectrometer with a DTGS detector in transmission mode at a resolution of 2 cm^{-1}. The samples were pressed into self-supporting wafers (ca. 10 mg/cm^2) and placed in a quartz cell sealed with $NaCl_2$ windows. The calcined sample was pretreated in an O_2 flow. The high-temperature-treated sample was pretreated in a flow of N_2 at 773 K for 1 h. The samples were cooled to RT in the same flow, followed by a N_2 purge for 20 min. Subsequently, the in situ pretreated sample was exposed to 1 vol% NO in He at a flow rate of 60 mL/min for 10 min and then purged with N_2 at a flow rate of 60 mL/min for 10 min. Spectra were collected as a function of exposure time or purging time. In all experiments, a reference spectrum collected before exposure to NO was subtracted from the spectra of NO adsorption. The overtones of zeolite lattice (1500–2000 cm^{-1}) of the reference spectrum was also used to normalize the spectra of various samples, enabling quantitative comparison of the number of Brønsted acid site as well as the number of NO_x groups after NO adsorption.

UV–vis diffuse reflectance spectra were recorded on a JASCO V-550 UV–vis spectrometer under ambient conditions. $BaSO_4$ was used as a reference material.

2.3. N_2O decomposition

A single-pass plug-flow quartz reactor with an inner diameter of 4 mm was used for N_2O decomposition. A 50-mg catalyst sample was retained between two quartz wool plugs. Pretreatment consisted of exposure to O_2 at 823 K (Fe/ZSM-5(C)) or He at 1173 K (Fe/ZSM-5(HT)) for 1 h. During steady-state catalytic measurements, the nitrous oxide concentration was 5.0% and the gas hourly space velocity was kept at 24,000 mL/(h g). A well-calibrated on-line mass spectrometer (Gam 200; Pfeiffer Vacuum) was used for quantification of gaseous products.

For transient-response experiments, a combination of a four-port switching valve and a six-port switching valve installed before the reactor allowed a step change in the gas-phase nitrous oxide concentration or a pulse of nitrous oxide. All transient-response experiments were performed after steady-state N_2O decomposition was reached. A typical transient-response experiment was performed by changing the nitrous oxide concentration from 5 vol% N_2O in He to pure He, or by pulsing 230 µL of 5 vol% N_2O–He mixture in a pure He flow or in a flow of 1 vol% N_2O in He.

3. Results

3.1. Steady-state N_2O decomposition

The steady-state conversion of nitrous oxide as a function of the reaction temperature over Fe/ZSM-5(C) and Fe/ZSM-5 (HT) is shown in Fig. 1. Fe/ZSM-5(C) calcined at 823 K

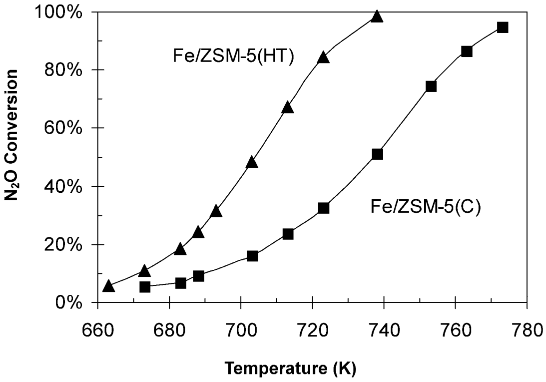

Fig. 1. Steady state N_2O conversion as a function of temperature over Fe/ZSM-5(C) and Fe/ZSM-5(HT). Feed: 5 vol% N_2O in He.

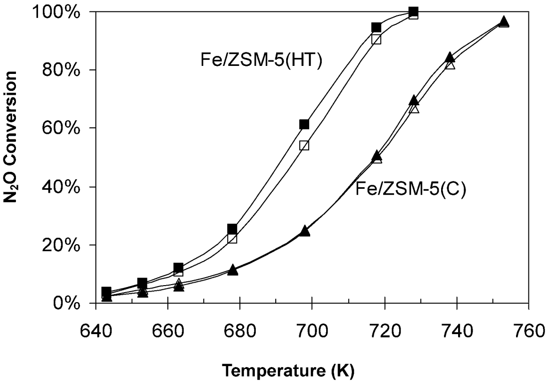

Fig. 2. Effect of gaseous O_2 on N_2O decomposition over (△, ▲) Fe/ZSM-5(C) and (◇, ◆) Fe/ZSM-5(HT). Feed for open symbols: 2 vol% N_2O + 1.2 vol% O_2 in He. Feed for solid symbols, 2 vol% N_2O in He.

shows a substantial conversion above 700 K. High-temperature treatment strongly improves the catalytic performance. Typically, the temperature to reach a conversion of 50% is lowered by almost 50 K. The effect of molecular oxygen on the rate of N_2O decomposition is shown in Fig. 2. The presence of molecule O_2 in the feed has little effect on N_2O conversion on the calcined Fe/ZSM-5(C), and noticeably inhibits N_2O conversion on Fe/ZSM-5(HT). Kinetic parameters for Fe/ZSM-5(C) and Fe/ZSM-5(HT) catalyst have been calculated from Arrhenius plots under the assumption of first-order disappearance of nitrous oxide [8,10–12]. Both the apparent activation energy E_{act} and the pre-exponential factor A are substantially higher after high-temperature treatment (Table 1), the apparent activation energy increases from 144 kJ/mol on Fe/ZSM-5(C) to 192 kJ/mol on Fe/ZSM-5(HT), and the pre-exponential factor A increases from 5.6×10^4 to 6.7×10^8 $\mathrm{mol_{N_2O}/(s\,mol_{Fe}\,Pa_{N_2O})}$. The increases in these kinetic parameters are in line with earlier observations by Zhu et al. [11], who found apparent activation energies of 136–151 kJ/mol for calcined Fe/ZSM-5 and 186–213 kJ/mol after calcination or steaming at 923 K. The values on the Fe/ZSM-5(HT) also agree well with those reported by of Bell et al. on the hydrothermal synthesized Fe/ZSM-5 followed by pretreatment in He at 1173 K [10].

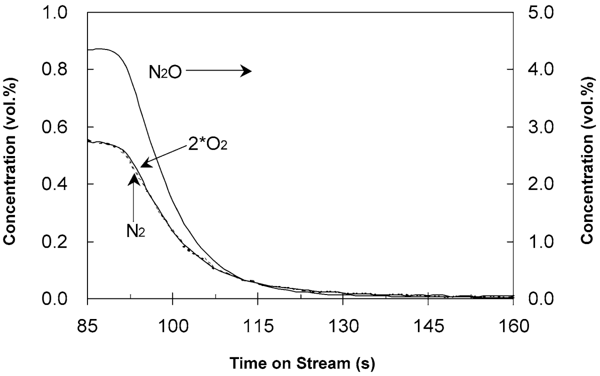

Fig. 3. Response of step change of 5 vol% N_2O in He to He flow at 698 K over Fe/ZSM-5(C).

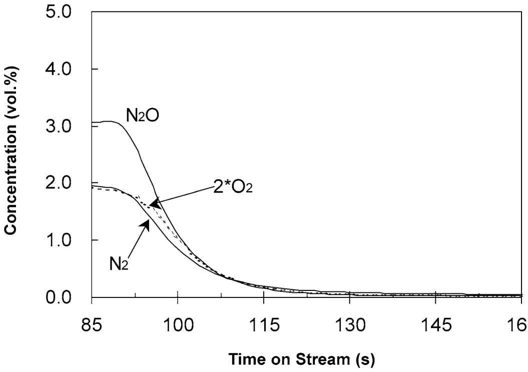

Fig. 4. Response of step change of 5 vol% N_2O in He to He flow at 698 K over Fe/ZSM-5(HT).

3.2. *Transient-response experiment*

3.2.1. *Step-response experiment*

All transient-response experiments were performed after the steady-state N_2O conversion was obtained. Fig. 3 shows the response after a step change in the nitrous oxide concentration from 5 vol% N_2O in He to pure He flow at 698 K over Fe/ZSM-5(C). The step results in a concomitant decrease of the gas-phase concentrations of N_2O, O_2, and N_2. The reaction stoichiometry of $N_2/O_2 = 2$ during the transient is maintained. However, Fig. 4 clearly shows that Fe/ZSM-5(HT) behaves differently: excess molecular oxygen is produced for a short time. Similar responses after the step change were obtained at 673 or 753 K.

3.2.2. *Pulse-response experiment on Fe/ZSM-5(C)*

The first step during catalytic nitrous oxide decomposition over Fe/ZSM-5 is thought to be the formation of surface oxygen on a free Fe site. The deposited surface oxygen can react with a second N_2O molecule or recombine with a neighboring surface oxygen atom to form O_2. To discriminate between these two alternative reaction pathways, pulse-response experiments were performed by pulsing N_2O in a flow of 1 vol% N_2O in He under steady-state conditions of catalytic nitrous oxide decomposition or in a flow of He.

Fig. 5 displays the response to a pulse of 5 vol% N_2O in a flow of 1 vol% N_2O over Fe/ZSM-5(C). Clearly, the evolution

Table 1
Activation energies (E_a) and pre-exponential factor (A) for N_2O decomposition to N_2 and O_2 over Fe/ZSM-5 catalysts

Sample[a]	Fe (wt%)	Pretreatment	E_a (kJ/mol)	A ($mol_{N_2O}/(s\,mol_{Fe}\,Pa_{N_2O})$)	Reference
Fe/ZSM-5(0.66)	2.4	823 K, O_2	144	5.6×10^4	This work
Fe/ZSM-5(1.1)[b]	4.5	773 K, He	139	1.8×10^6	[25]
Fe/ZSM-5(0.97)	3.6	823 K, O_2	136	–	[11]
Fe/ZSM-5(0.66)	2.4	1173 K, He	192	6.7×10^8	This work
Fe/ZSM-5(0.97)	3.6	973 K, O_2	186	–	[11]
Fe/ZSM-5(0.97)	3.6	973 K, steaming	195	–	[11]
Fe/ZSM-5(0.38)[c]	0.38	1123 K, He	185	9.9×10^8	[10]

[a] Sample is designated as Fe/ZSM(x), where x indicates the Fe/Al ratio.
[b] The pre-exponential factor is calculated by the rate constant at 698 K.
[c] Fe/ZSM-5 is prepared by isomorphous substitution method.

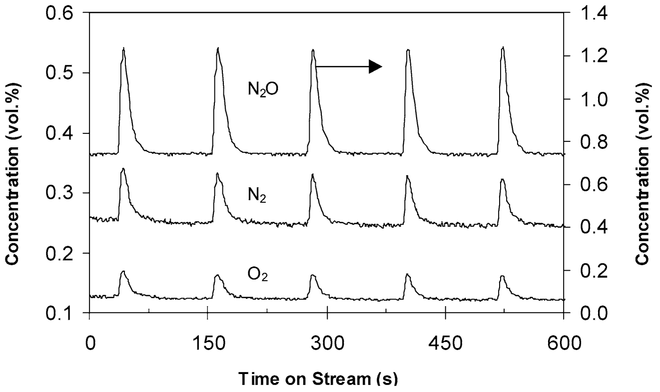

Fig. 5. Response of N_2O pulse into 1 vol% N_2O in He flow at 698 K under steady state N_2O decomposition over Fe/ZSM-5(C).

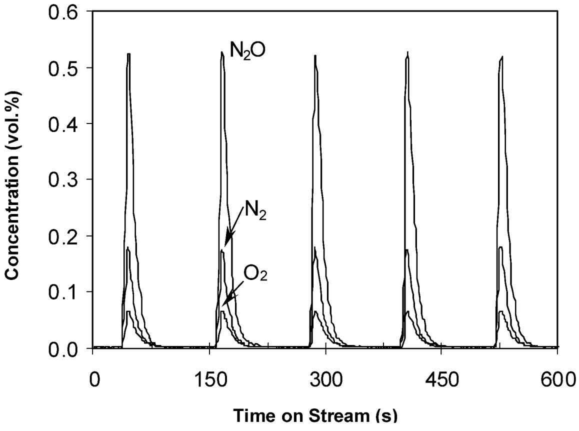

Fig. 6. Response of N_2O pulse into He flow at 698 K over Fe/ZSM-5(C).

of molecular oxygen and nitrogen due to the increased nitrous oxide concentration follows the pulse of nitrous oxide. A pulse of 5 vol% N_2O in a flow of He over Fe/ZSM-5(C) shows similar behavior, and the nitrous oxide is partly consumed, instantaneously giving stoichiometric amounts of nitrogen and oxygen (Fig. 6). A series of five pulses produced no indication of deactivation. Pulse-response experiments conducted at lower temperature (673 K) or at higher temperature (753 K) also gave similar results. Thus, we conclude that Fe/ZSM-5(C) produces equivalent amounts of nitrogen and oxygen on decomposition of nitrous oxide during pulse-response experiments.

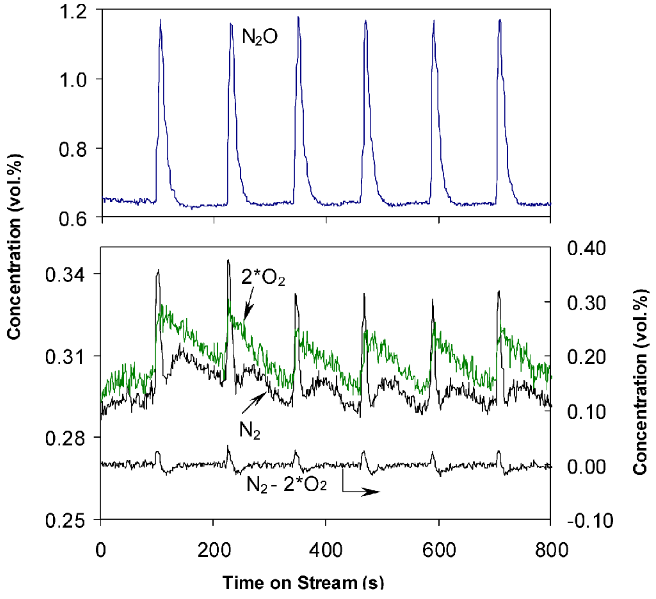

Fig. 7. Response of N_2O pulse into 1 vol% N_2O in He flow at 698 K under steady state N_2O decomposition over Fe/ZSM-5(HT).

3.2.3. Pulse-response experiment on Fe/ZSM-5(HT)

The response to a pulse of nitrous oxide under conditions of steady-state nitrous oxide decomposition is more complex (Fig. 7). First, the evolution of oxygen is evolved for about 2 min, obviously delayed compared with those of nitrous oxide and nitrogen, whereas the width of the main nitrogen production peak is close to the width of the nitrous oxide pulse. Second, two nitrogen production peaks are observed, a distinct main peak following the nitrous oxide pulse and a smaller and more diffuse second peak. Fig. 7 also displays the difference curve for the excess nitrogen (deficit oxygen) observed in the gas-phase based on the reaction stoichiometry of $N_2/O_2 = 2$. A sharp positive peak followed by a broad negative peak is observed on the difference curve, suggesting that oxygen formation is delayed. Moreover, at the time for second nitrogen peak, the value of the difference curve is close to zero and a small drop in nitrous oxide concentration is observed. These observations suggest that the second N_2 peak is due to the enhanced N_2O conversion as a result of the disturbance of the surface by a N_2O pulse. Performing the pulse-response experiments at lower (678 K) or higher temperature (723 K) will

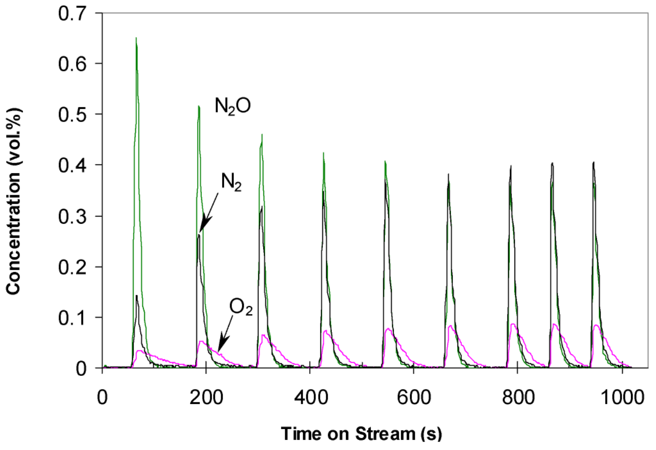

Fig. 8. Response of N_2O pulse into He flow at 698 K over Fe/ZSM-5(HT).

flatten or sharpen the evolution of molecular oxygen, respectively. This suggests that oxygen formation is slower (faster) at lower (higher) temperatures.

Fig. 8 shows the response of a nitrous oxide pulse over Fe/ZSM-5(HT) kept in He. Again, we observe that the evolution of molecular oxygen is delayed compared with those of N_2O and N_2. The O_2 evolution has a very broad feature; even after the concentration of N_2O and N_2 decreases to zero, the evolution of O_2 continues and lasts for about 100 s. Another important observation is that the conversion of nitrous oxide during consecutive pulses increases until a steady-state conversion per pulse is attained.

Table 2 shows further data derived from this pulse-response experiment for Fe/ZSM-5(HT). Most notably, O_2 is produced in excess of N_2 during the first pulses. This oxygen excess gradually decreases during the consecutive pulses until after the seventh pulse the nitrous oxide per pulse decomposes stoichiometrically. The origin of this behavior must be related to the presence of oxygen species on the surface, derived from the decomposition of nitrous oxide during the previous steady-state catalytic nitrous oxide decomposition.

The nitrous oxide conversion per pulse is also given in Table 2. Because not all molecular oxygen comes from nitrous oxide in the pulse, the nitrous oxide conversion is based on its decomposition in molecular nitrogen. The conversion gradually increases from 21% to about 55%. This increased conversion is concomitant with the removal of the surface oxygen: once the O_2 excess becomes very small (i.e., no more surface oxygen can be extracted by new N_2O pulses), the conversion also approaches its maximum value.

Table 2
Quantified response of N_2O pulse in He flow over Fe/ZSM-5(HT) at 698 K

Pulse No.	Amount (10^{-2} mol/mol$_{Fe}$) N_2O	O_2	N_2	O_2 excess[a] (10^{-2} mol/mol$_{Fe}$)	N_2O conversion[b] (%)
1	5.82	1.24	1.55	0.466	21.0
2	4.64	1.53	2.71	0.175	36.8
3	4.15	1.68	3.16	0.103	43.7
4	3.91	1.79	3.44	0.073	46.8
5	3.72	1.88	3.61	0.073	49.3
6	3.39	1.93	3.71	0.072	52.3
7	3.24	1.96	3.82	0.050	54.1
8	3.17	1.98	3.94	0.010	55.4
9	3.19	1.97	3.94	0	55.3

[a] O_2 excess is expressed by $A_{O_2} - (A_{N_2}/2)$.

[b] N_2O conversion in each pulse is calculated by $A_{N_2}/(A_{N_2} + A_{N_2O})$.

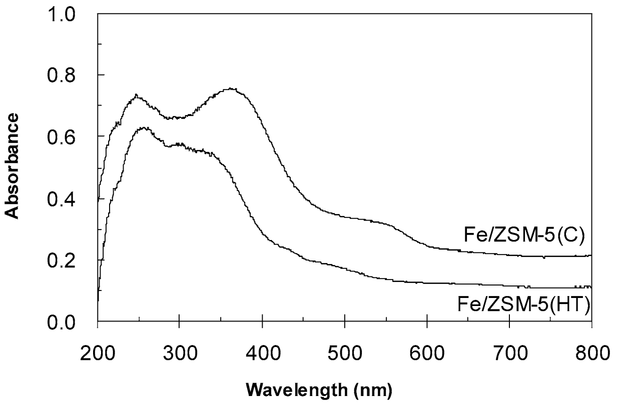

Fig. 9. UV–vis diffuse reflectance spectra of Fe/ZSM-5(C) and Fe/ZSM-5(HT).

3.3. *Characterization of iron species*

Fig. 9 displays the UV–vis diffuse reflectance spectra for Fe/ZSM-5(C) and Fe/ZSM-5(HT). The spectrum of Fe/ZSM-5(C) exhibits two intense bands at 245 and 350 nm and a weak band at 500–600 nm. Bands between 200 and 300 nm are generally attributed to LMCT (oxygen to iron) transitions of isolated Fe^{3+} species, either tetrahedrally coordinated in framework or extra-framework positions or octahedrally coordinated in extra-framework positions [17,28,29]. Here the band at 245 nm is attributed to isolated Fe^{3+} species at extra-framework positions, which is derived from the fact that the catalysts have been prepared by solid-state ion exchange. Octahedral ferric species in small oligonuclear clusters are characterized by strong absorptions between 300 and 400 nm, whereas bands at higher wavelengths are typically attributed to Fe^{3+} ions in iron oxide aggregates [17,18,28,29]. The UV–vis spectrum of Fe/ZSM-5(C) thus indicates the presence of ferric ions as isolated ions, in oligonuclear iron clusters, and in bulk iron oxide aggregates.

After high-temperature treatment, the absorption band at 245 nm sharpens, and the band at 350 nm assigned to oligonuclear species and the band at 550 nm due to more clustered iron oxides decrease substantially. Weak absorptions appear at 292, 430, and 475 nm. The origins of these new absorptions are unknown. However, it has been reported that isolated Fe^{3+} in the octahedral sites of alumina exhibit a band at 286 nm [28]. Bands at 280–300 nm have been reported for steamed FeAlMFI catalysts [26,30]. These observations indicate that the nature of the iron sites becomes profoundly modified after heating in He at 1173 K.

Iron speciation was further studied by infrared spectroscopy. Fig. 10 displays the hydroxyl-stretching region of the infrared spectra for Fe/ZSM-5(C) and Fe/ZSM-5(HT), along with the spectrum of the parent zeolite for comparison. Bands at 3610 cm^{-1}, related to the stretching vibration of the Brønsted acid bridging hydroxyl group, and at 3740 cm^{-1}, related to

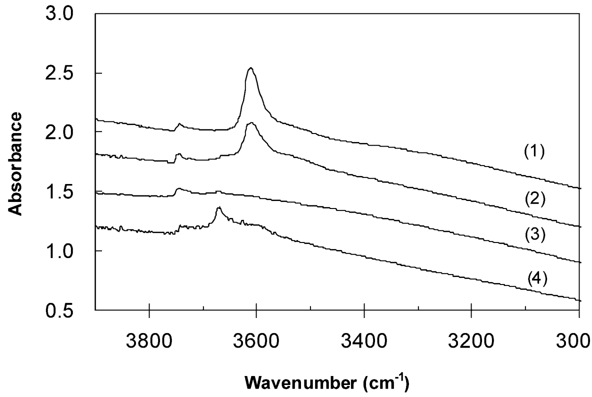

Fig. 10. Infrared spectra of the hydroxyl-stretching region: (1) H-ZSM-5; (2) Fe/ZSM-5(C); (3) Fe/ZSM-5(HT); (4) after hydration of Fe/ZSM-5(HT).

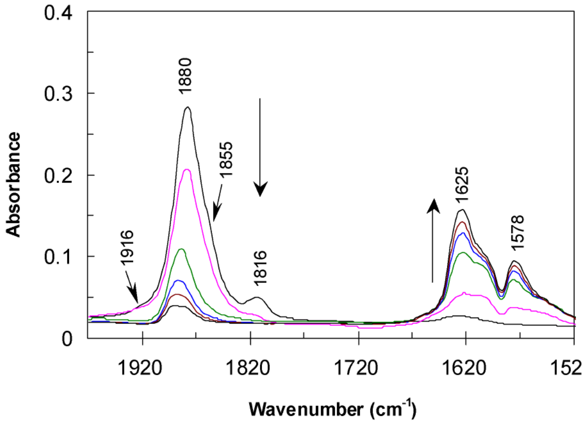

Fig. 11. Infrared spectra of NO adsorption on Fe/ZSM-5(C) at RT. From top to bottom: NO 10 min, after N_2 purge for 1, 3, 5, and 10 min.

silanol groups, are observed for H/ZSM-5 and Fe/ZSM-5(C). The intensity of the band at 3610 cm^{-1} is much weaker for Fe/ZSM-5(C) than for H/ZSM-5, suggesting the replacement of a considerable portion of the Brønsted acid groups by cationic iron species. Once the sample is treated in He at 1173 K, the band of the Brønsted acid groups at 3610 cm^{-1} disappears. The decreased Brønsted acidity is mainly due to the extensive extraction of the aluminum from a framework to an extra-framework position, because rehydration of the sample resulted in only a very slight recovery of the signal at 3610 cm^{-1} and the appearance of a strong band at 3670 cm^{-1} associated with the hydroxyl group connected to aluminum in an extra-framework position [31,32].

Fig. 11 shows infrared spectra of NO adsorbed on Fe/ZSM-5(C), along with the dynamics of the infrared bands related to NO on N_2 purge. A strong band at 1880 cm^{-1} with a weak shoulder at 1855 cm^{-1} and weak bands at 1916 and 1816 cm^{-1} are observed after exposing the sample to 1 vol% NO in He. The bands at 1880 and at 1858 cm^{-1} are very similar to those observed for sublimed Fe/ZSM-5 and Fe/ZSM-5 prepared by solid-state ion exchange after oxidative pretreatment at 823 K [33–35]. The bands in this region are quite sensitive to the location and nature of iron sites. Sachtler et al. [33] and Bell et al. [34] assigned the doublet at 1876 and 1852 cm^{-1} to mono-nitrosyl species on iron sites located at different positions, that is, the five-and six-membered rings of the zeolite crystal, respectively. Mul et al. [37] and Spoto et al. [36] also observed the band at around 1850 cm^{-1} for steamed Fe-silicalite and ascribed it to mono-nitrosyl groups on oligonuclear iron species. The bands at 1916 and 1816 cm^{-1} are normally assigned to di-nitrosyl on isolated Fe^{2+} site located at a readily accessible position, the main channel with 10-membered ring in the ZSM-5 crystal [33–35,37]. Spoto et al. [36] assigned these bands to tri-nitrosyl on isolated Fe^{2+} sites.

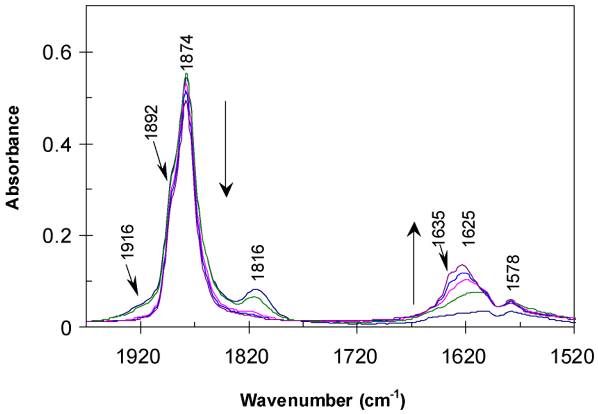

Fig. 12. Infrared spectra of NO adsorption on Fe/ZSM-5(HT) at RT. From top to bottom: NO 10 min, after N_2 purge for 1, 3, 5, and 10 min.

On purging with N_2, the bands of poly-nitrosyl (di-nitrosyl or tri-nitrosyl) groups at 1916 and 1816 cm^{-1} quickly disappear, followed by the disappearance of the bands at 1882 and 1852 cm^{-1}. New absorptions at 1578 and 1625 cm^{-1} with a shoulder at 1600 cm^{-1} gradually develop. The bands at 1625 and 1600 cm^{-1} have been assigned to NO_2 adsorbed on iron oxide species, whereas the band at 1578 cm^{-1} is generally assigned to a nitrate group [33,34].

The infrared spectra of NO adsorbed on Fe/ZSM-5(HT) are collected in Fig. 12. Weak absorptions of poly-nitrosyl on isolated Fe^{2+} site at 1916 and 1816 cm^{-1}, as well as a strong band at 1874 cm^{-1} with a shoulder at 1892 cm^{-1}, are observed. Purging with N_2 results in rapid desorption of the poly-nitrosyl groups, with only a slight decrease in the bands at 1874 and 1892 cm^{-1}. Along with the appearance of absorption bands of nitro and nitrate groups at 1625 and 1600 cm^{-1}, respectively, similar to Fe/ZSM-5(C), a new band at 1635 cm^{-1} gradually develops during N_2 purging. Although the high-temperature treatment apparently does not affect the di-nitrosyl or poly-nitrosyl bands at 1916 and 1816 cm^{-1}, the shape of the doublet at around 1880 cm^{-1} changes drastically. Mul et al. [37] reported a similar doublet, composed of a strong band at 1874 cm^{-1} with a shoulder at 1892 cm^{-1}, for steamed [Fe, Al] MFI and attributed it to NO adsorbed on extra-framework Fe–O–Al species. They also found that replacing Al with Ga shifts the doublet to 1867 and 1881 cm^{-1}. The strong band at 1874 cm^{-1} observed for Fe/ZSM-5(HT) is accordingly assigned to NO adsorption on extra-framework Fe–O–Al species. The band at 1892 cm^{-1} has been assigned to mono-nitrosyl on isolated iron or oligonuclear iron species [34]. But because this band is sensitive to the replacement of Al with Ga [37], and because it exhibits similar dynamic behavior to the band at 1874 cm^{-1} on purging, it is more likely to be also associated with some kinds of extra-framework Fe–O–Al species. The appearance of a band at 1635 cm^{-1} coheres with the earlier findings [37,38] of the formation of NO_2 species that are adsorbed to extra-framework Fe–O–Al species.

4. Discussion

4.1. Different mechanisms of N_2O decomposition on Fe/ZSM-5(C) and Fe/ZSM-5(HT)

The distinctly different behaviors of Fe/ZSM-5(C) and Fe/ZSM-5(HT) in the transient-response activity measurements suggests that nitrous oxide is decomposed by different mechanisms. A step change to inert gas during steady-state nitrous oxide decomposition was applied to probe the mechanism of N_2O decomposition on MnO_2 [39]. It was found that removing N_2O from the feed led to an instantaneous end to the evolution of N_2, whereas the evolution of O_2 continued for several minutes. From such observations, it was concluded that oxygen apparently evolves by recombination of atomic oxygen species over MnO_2 [39]. Similar experiments for Fe/ZSM-5(C) and Fe/ZSM-5(HT) have shown that for the latter material, O_2 evolves after a short delay, suggesting that for Fe/ZSM-5(HT), molecular oxygen is formed by recombinative oxygen desorption. In obvious contrast with this behavior, oxygen and nitrogen are produced simultaneously over Fe/ZSM-5(C). This points to the importance of evolution of oxygen due to a direct reaction of adsorbed oxygen with a gas-phase nitrous oxide molecule. The pulse-response experiments support this conjecture. For Fe/ZSM-5(C), the signals of molecular nitrogen and oxygen evolve simultaneously. This is valid for nitrous oxide pulses during steady-state nitrous oxide decomposition, as well as during exposure to an inert helium flow.

Previous isotopic exchange experiments [25,41,42] are relevant to the mechanism of N_2O decomposition on Fe/ZSM-5(C). The study by Nobukawa et al. [42] on liquid ion-exchanged Fe/ZSM-5 followed by calcinations at 773 K revealed that the ^{18}O fraction in the produced O_2 is about half the value of that on the surface, suggesting that the oxygen atom deriving from decomposition of a first nitrous oxide molecule is removed via a scavenging mechanism by a second nitrous oxide molecule. This is in line with the mechanism on the present calcined catalyst, as well as with that suggested by Kapteijn on catalyst prepared by liquid ion exchange followed by calcinations in 873 K [8]. However, the isotopic exchange study by Pirngruber et al. [25,41] on Fe/ZSM-5 prepared by CVD of $FeCl_3$ followed by calcinations at 773 K found very rapid scrambling of oxygen suggesting that there is a pool of oxygen atoms from which molecular oxygen desorbs via slow recombination. This finding contrasts with our results for the present calcined material. Nevertheless, Pirngruber et al. [41] also found that for a similar catalyst prepared by ion exchange, scrambling was not complete, suggesting that a different mechanism is operating. We note that we cannot firmly define the mechanism on the calcined Fe/ZSM-5(C), because in principle it is also possible that another step than oxygen desorption is rate-limiting—as has been suggested by recent DFT calculations of N_2O decomposition on cationic iron sites [40]—although it is generally accepted that oxygen removal is the rate-determining step [8–13]. Systematic isotopic scrambling experiments are needed to gain more insight into these differences.

The transient behavior of Fe/ZSM-5(HT) is very different. The pulse-response experiments show that molecular nitrogen evolves simultaneously with the nitrous oxide pulse, whereas evolution of molecular oxygen is delayed. The evolution of oxygen is more diffuse and lasts for longer than 1 min, even when gaseous N_2O has depleted and the production of nitrogen has stopped. We attribute these different transient behaviors to differences in the mechanism of oxygen removal. For Fe/ZSM-5(C), the oxygen atom deriving from the decomposition of a first nitrous oxide molecule is removed via a scavenging mechanism by a second nitrous oxide molecule. In contrast, the behavior of Fe/ZSM-5(HT) points to recombination of adsorbed oxygen species to molecular O_2 as the slowest step in the mechanism. The differences in rate-limiting step and/or mechanism are also consistent with the strong differences in apparent activation energies. We once again note that the activity of Fe/ZSM-5(C) is much lower than that of Fe/ZSM-5(HT).

Additional support for our view is provided by our finding that molecular oxygen decreases the catalytic activity of the high-temperature-treated catalyst. The activity of Fe/ZSM-5(C) is not affected by the presence of molecular oxygen; however, the rate over Fe/ZSM-5(HT) is suppressed by the presence of oxygen (Fig. 2). This indicates that the recombinative desorption of surface oxygen is reversible, and hence oxygen acts as a poison to the catalytic reaction.

Interestingly, we find that nitrous oxide pulses in He flow extract surface oxygen species from Fe/ZSM-5(HT). Clearly, these species do not derive from a reaction between adsorbed oxygen and gas-phase nitrous oxide, because the evolution of oxygen is very diffuse. The adsorbed oxygen species are present because, before being exposed to the inert He flow, the catalyst was used in steady-state nitrous oxide decomposition. Because the removal of surface oxygen is rate-determining [8–12], the catalytic surface is occupied by oxygen atoms. When the feed of nitrous oxide is stopped, a relatively small amount of oxygen desorbs, as evidenced by the tailing O_2 desorption in the step-response experiment on Fe/ZSM-5(HT) (Fig. 4). The density of the remaining surface oxygen atoms may be quite high, and these atoms do not recombine and desorb as oxygen, possibly because they are spatially separated. This is in line with oxygen desorption being rate-limiting for this catalyst. The oxygen atoms provided by decomposition of nitrous oxide in a pulse recombine with oxygen atoms already present on the surface. This explains the excess oxygen observed during pulsing of nitrous oxide for Fe/ZSM-5(HT). Eventually, these oxygen atoms are all stripped of the surface, and the decomposition reaction of the pulses becomes stoichiometric. This implies that the number of vacant sites increases during pulsing of nitrous oxide, and indeed it is observed that the nitrous oxide conversion based on the amount of evolved nitrogen increases.

4.2. Different iron speciation on Fe/ZSM-5(C) and Fe/ZSM-5(HT)

The heterogeneous nature of iron species in Fe/ZSM-5 catalysts has been studied extensively [13–22]. On the present Fe/ZSM-5(C) isolated mono-nuclear iron species, small oligonuclear iron clusters and more bulky iron oxide aggregates are identified by UV–vis spectroscopy. Absorption above 300 nm in the UV–vis spectrum of Fe/ZSM-5(C) is quite extensive, indicating the broad and heterogeneous distribution of the iron clusters. The infrared spectra of NO adsorption on Fe/ZSM-5(C) further reveal that a broad range of species is present. Most notably, large fractions of iron species are compensating for the negative framework charge of the zeolite. High-temperature treatment profoundly modifies the nature of the iron species. UV–vis spectra show that the band at 245 nm on Fe/ZSM-5(HT) sharpens. The broad band at 350 nm for Fe/ZSM-5(C) related to oligonuclear iron clusters decreases substantially. The infrared spectra provide more detailed information. Extensive extraction of framework aluminum to an extra-framework position is observed after high-temperature treatment. Both spectra of NO adsorption on Fe/ZSM-5(C) and Fe/ZSM-5(HT) show bands (1916 and 1816 cm^{-1}) due to dinitrosyl on isolated highly accessible Fe sites. These observations suggest that the nature of the isolated iron species located in highly accessible positions on Fe/ZSM-5(C) are not modified by high-temperature treatment. In contrast, high-temperature treatment changed the structure of the isolated or oligonuclear iron species that give rise to bands at around 1880 cm^{-1}. The doublet at 1882 and 1855 cm^{-1} in the spectra of Fe/ZSM-5(C), due to the isolated or oligonuclear iron species in the five- or six-membered rings, are replaced by a doublet at 1874 and 1892 cm^{-1} that is typical for adsorption of NO on extra-framework Fe–O–Al species. This is further supported by the appearance of a band at 1635 cm^{-1} assigned to NO_2 species on extra-framework Fe–O–Al moieties.

The above findings suggest that the cationic iron species that initially compensate for the negative framework charge of the aluminium-occupied oxygen tetrahedron are transformed into extra-framework Fe–O–Al species. It could well be that these species are then located in the channels of the zeolite and stabilized by the micropores of the zeolite support. Recently, it has been proposed that such extra-framework Fe–O–Al species might be responsible for the decomposition of nitrous oxide at low temperature, that is, formation of so-called "α-oxygen" [18,24] as an alternative to the original model of a mononuclear or binuclear charge-compensating iron species. The activity in phenol formation from benzene with nitrous oxide appears to be related to the amount of Fe–O–Al species [18,38]. We note that such extra-framework Fe–O–Al species might be quite heterogeneous in nature, because they apparently are formed from a broad range of other iron species, including even more clustered species. In this respect, it is noteworthy that Zhu et al. [43] suggested that at higher temperatures, a protolysis reaction between neutral iron oxide clusters and protons leads to increased cationic iron species and a concomitant activity increase in nitrous oxide decomposition.

4.3. The active sites for N_2O decomposition

The results of the transient-response experiments point strongly to different operative mechanisms for Fe/ZSM-5 catalysts before and after high-temperature treatment. Steady-state N_2O decomposition provides important information on the nature of the active site. The rate-determining step for nitrous oxide decomposition is the removal of surface oxygen atoms [8–13]. The change in the mechanism of oxygen removal from reaction with a gaseous nitrous oxide molecule to recombination of surface oxygen atoms is reflected in the change in the apparent activation energy. The different values are more difficult to explain. In any case, the apparent activation energy for the recombinative case should be the true activation energy for oxygen removal, because the surface is considered fully occupied. The activation energy may be lower for Fe/ZSM-5(C) because a different mechanism is operative or a different step than oxygen desorption in the same mechanism is rate-limiting. This difference most likely stems from the differing nature of iron sites. Similarly, the strong increase in the pre-exponential factor from $5.6 \times 10^4\ \text{mol}_{N_2O}/(\text{s}\,\text{mol}_{Fe}\,\text{Pa}_{N_2O})$ (Fe/ZSM-5(C)) to $6.7 \times 10^8\ \text{mol}_{N_2O}/(\text{s}\,\text{mol}_{Fe}\,\text{Pa}_{N_2O})$ (Fe/ZSM-5(HT) may reflect the high entropy gain during the recombinative desorption of oxygen compared with the much smaller entropy gain in the former case (which involves a gaseous molecule). This difference also could be due in part to the higher number of active sites in the latter case. In summary, the kinetic parameters provide strong evidence that different sites are involved for nitrous oxide decomposition over Fe/ZSM-5(C) and Fe/ZSM-5(HT).

Combining this notion with the results of catalyst characterization suggests that these changes are due to the transformation of cationic and/or neutral clustered iron species to extra-framework Fe–O–Al species upon high-temperature treatment. It is well known that bulky iron oxides do not participate in nitrous oxide decomposition under the present reaction conditions. Pérez-Ramírez et al. [17] showed that N_2O decomposition is favored over oligonuclear iron species and is more difficult over isolated iron sites. The present infrared spectra of NO adsorption reveal the presence of similar isolated iron species located at the highly accessible positions of zeolite crystal for both Fe/ZSM-5(C) and Fe/ZSM-5(HT). In contrast, the charge-compensating species in the five- and six-membered rings disappear on such treatment. Thus, the involvement of different active sites before and after high-temperature treatment appears related to the transformation of cationic iron clusters in Fe/ZSM-5(C) to extra-framework Fe–O–Al species on Fe/ZSM-5(HT). A fraction of the neutral iron oxide clusters may also be transformed by first reacting with the protons at high temperature to give cationic Fe species [43], whereupon the tetrahedral Al atoms are extracted to extra-framework positions to form Fe–O–Al species.

We suggest that nitrous oxide decomposition occurs mainly on more clustered iron clusters in Fe/ZSM-5(C). The surface oxygen on oligonuclear iron clusters is removed by reaction with a gaseous N_2O molecule. A less likely explanation is that oxygen desorption is facile because the degree of coordinative unsaturation is probably not high. For nitrous oxide decomposition over Fe/ZSM-5(HT), the proposed active sites are extra-framework Fe–O–Al species. The surface oxygen atoms are removed by recombination of adsorbed oxygen atoms. The kinetic parameters suggest that the higher activity of Fe/ZSM-5 (HT) is related to a much higher intrinsic reactivity of the Fe–O–Al species, although this cannot be firmly concluded without further estimation of the active site density. Tentatively, the decomposition may proceed over coordinatively unsaturated Fe^{3+} ions in clustered iron species in Fe/ZSM-5(C), whereas it is catalyzed by Fe^{2+} sites stabilized by extra-framework Al in Fe/ZSM-5(HT). The importance of extra-framework Al in stabilizing Fe^{2+} sites is also supported by our recent finding that the number of Fe^{2+} sites, as well as the rate of N_2O decomposition over Fe/ZSM-5, increase on addition of Al [24].

5. Conclusion

High-temperature treatment of Fe/ZSM-5 prepared by solid-state ion exchange profoundly changes the iron speciation. Spectroscopic measurements indicate that clustered iron oxide and cationic iron species are transformed in mixed iron and aluminium oxide species. These changes on high-temperature treatment are concomitant with a significant increase in the rate of catalytic nitrous oxide decomposition. Moreover, the kinetic parameters for calcined and high-temperature-treated catalysts differ strongly, pointing to a different reaction mechanism. This latter point is corroborated by transient-response experiments showing that oxygen removal proceeds by recombinative oxygen desorption for the high-temperature-treated catalyst, whereas reaction of adsorbed oxygen species with gaseous nitrous oxide leads to molecular oxygen for the calcined one. This is in line with the finding that only the reaction over the high-temperature-treated catalyst is inhibited by molecular oxygen.

We propose that nitrous oxide decomposition over calcined Fe/ZSM-5 is catalyzed by clustered iron species, most likely by coordinatively unsaturated Fe^{3+} sites. The reaction proceeds at a low rate because in a scavenging-type (Eley–Rideal) mechanism, a deposited oxygen atom reacts with gas-phase nitrous oxide. Upon high-temperature treatment, a new type of active site—Fe^{2+} sites stabilized by extra-framework Al species in the micropore of zeolite—is formed. These sites are able to decompose nitrous oxide at a higher rate. The rate-limiting step becomes the recombinative desorption of molecular oxygen.

Acknowledgments

This work was supported by the Chinese National Basic Research Program (grants 203CB615806 and 2004CB720607), the Program for Strategic Scientific Alliances Between China and The Netherlands, and the Chinese National Natural Science Foundation (grant 20273069).

References

[1] H. Rodhe, Science 248 (1990) 1217.
[2] G. Centi, S. Perathoner, F. Vanazza, Chem. Tech. 12 (1999) 48.
[3] G. Centi, S. Perathoner, F. Vanazza, M. Marella, M. Tomaselli, M. Mantegazza, Adv. Environ. Res. 4 (2000) 325.
[4] J. Pérez-Ramírez, F. Kapteijn, G. Mul, J.A. Moulijn, Chem. Commun. (2001) 693.
[5] J. Pérez-Ramírez, F. Kapteijn, G. Mul, J.A. Moulijn, Appl. Catal. B 35 (2002) 227.
[6] G.I. Panov, A.K. Uriarte, M.A. Rodkin, V.I. Soblov, Catal. Today 41 (1998) 365.
[7] G.I. Panov, Cattech 4 (2000) 18.
[8] F. Kapteijn, G. Marbán, J. Rodriguez-Mirasol, J.A. Moulijn, J. Catal. 167 (1997) 256.
[9] G.D. Pirngruber, J. Catal. 219 (2003) 456.
[10] B.R. Wood, J.A. Reimer, A.T. Bell, M.T. Janicke, K.C. Ott, J. Catal. 224 (2004) 148.
[11] Q. Zhu, B.L. Mojet, R.A.J. Janssen, E.J.M. Hensen, J. Van Grondelle, P.C.M.M. Magusin, R.A. van Santen, Catal. Lett. 81 (2002) 205.
[12] G. Mul, J. Pérez-Ramírez, F. Kapteijn, J. Moulijn, Catal. Lett. 77 (2001) 7.
[13] J. Pérez-Ramírez, F. Kapteijn, G. Mul, J. Moulijn, J. Catal. 208 (2002) 211.
[14] L.J. Lobree, I.C. Hwang, J.A. Reimer, A.T. Bell, J. Catal. 186 (1999) 242.
[15] H.-Y. Chen, W.M.H. Sachtler, Catal. Today 42 (1998) 73.
[16] P. Fejes, K. Lázár, I. Marsi, A. Rockenbauer, L. Korecz, J.B. Nagy, S. Perathoner, G. Centi, Appl. Catal. A: Gen. 252 (2003) 75.
[17] J. Pérez-Ramírez, F. Kapteijn, A. Brückner, J. Catal. 214 (2003) 33.
[18] E.J.M. Hensen, Q. Zhu, M.M.R.M. Hendrix, A.R. Overweg, P.J. Kooyman, M.V. Sychev, R.A. van Santen, J. Catal. 221 (2004) 560.
[19] P. Marturano, L. Drozdova, A. Kogelbauer, R. Prins, J. Catal. 192 (2000) 236.
[20] M.S. Kumar, M. Schuwidder, W. Grünert, A. Brückner, J. Catal. 227 (2004) 384.
[21] G. Berlier, A. Zecchina, G. Spoto, G. Ricchiardi, S. Bordiga, C. Lamberti, J. Catal. 215 (2003) 264.
[22] J. Jia, K.S. Pillai, W.M.H. Sachtler, J. Catal. 221 (2004) 119.
[23] K.A. Dubkov, N.S. Ovanesyan, A.A. Shteinman, E.V. Starokon, G.I. Panov, J. Catal. 207 (2002) 341.
[24] K. Sun, H. Zhang, H. Xia, Y. Lian, Y. Li, Z. Chi, P. Ying, C. Li, Chem. Commun. (2004) 2480.
[25] P.K. Roy, G.D. Pirngruber, J. Catal. 227 (2004) 164.
[26] E.J.M. Hensen, Q. Zhu, R.A.J. Janssen, P.C.M.M. Magusin, P.J. Kooyman, R.A. van Santen, J. Catal. 233 (2005) 136.
[27] B. Sulikowski, J. Find, H.G. Karge, D. Herein, Zeolite 19 (1997) 395.
[28] S. Bordiga, R. Buzzoni, F. Geobaldo, C. Lamberti, E. Giamello, A. Zecchina, G. Leofanti, G. Petrini, G. Tozzola, G. Vlaic, J. Catal. 158 (1996) 486, and references therein.
[29] P. Marturano, L. Drozdova, G.D. Pirngruber, A. Kogelbauer, R. Prins, Phys. Chem. Chem. Phys. 3 (2001) 5585.
[30] J. Pérez-Ramírez, J. Catal. 227 (2004) 503.
[31] P.O. Fritz, J.H. Lunsford, J. Catal. 118 (1989) 85.
[32] S. Bordiga, E.E. Platero, C.O. Arean, C. Lamberti, A. Zecchina, J. Catal. 137 (1992) 179.
[33] H.-Y. Chen, E.M. Malki, X. Wang, R.A. van Santen, W.M.H. Sachtler, J. Mol. Catal. A: Chem. 162 (2000) 159.
[34] L.J. Lobree, I.C. Hwang, J.A. Reimer, A.T. Bell, Catal. Lett. 63 (1999) 233.
[35] R.W. Joyer, M. Stockenhuber, J. Phys. Chem. B 103 (1999) 5963.
[36] G. Spoto, A. Zecchina, G. Berlier, S. Bordiga, M.G. Clerici, L. Bisini, J. Mol. Catal. A: Chem. 158 (2000) 107.
[37] G. Mul, J. Pérez-Ramírez, F. Kapteijn, J. Moulijn, Catal. Lett. 80 (2002) 129.

[38] E.J.M. Hensen, Q. Zhu, R.A. van Santen, J. Catal. 233 (2005) 136.
[39] F. Kapteijn, J. Rodriguez-Mirasol, J. Moulijn, Appl. Catal. B 9 (1996) 25, and references therein.
[40] A. Heyden, B. Peters, A.T. Bell, F.J. Keil, J. Phys. Chem. B 109 (2005) 1857.
[41] G.D. Pirngruber, P.K. Roy, Catal. Lett. 93 (2004) 75.
[42] T. Nobukawa, S. Tanaka, S. Ito, K. Tomishige, S. Kameoka, K. Kunimori, Catal. Lett. 83 (2002) 5.
[43] Q. Zhu, E.J.M. Hensen, B.L. Mojet, J.H.M.C. van Wolput, R.A. van Santen, Chem. Commun. (2002) 1232.